# Deprotection Volume Characteristics and Line Edge Morphology in Chemically Amplified Resists

Ronald L. Jones[*a], Tengjiao Hu[a], Vivek M. Prabhu[a], Christopher L. Soles[a], Eric K. Lin[a], Wen-li Wu[a], Dario L. Goldfarb[b], Marie Angelopoulos[b], Brian C. Trinque[c], and C. Grant Willson[c]

[a]Polymers Division, National Institute of Standards and Technology, Gaithersburg, MD 20899
[b]IBM T.J. Watson Research Center, Yorktown Heights, NY 10598
[c]Department of Chemistry, University of Texas at Austin, Austin, TX 78712

## ABSTRACT

The form and magnitude of line edge roughness (LER) is increasingly important in semiconductor processing due to continued reductions in feature sizes. While a large body of work connects processing factors to LER magnitude, the spatial dependence of LER is needed to provide a more complete description. The distribution of deprotection within the resist is represented as a collection deprotection paths created by individual photoacid generators (PAGs). In the limit of dilute PAG concentration, the form and size of the average deprotection path is measured using Small Angle Neutron Scattering (SANS) for a model photoresist polymer and PAG mixture. The heterogeneity of the deprotection volume produces "fuzzy blobs". The shape of these blobs is compared to the form of LER at a idealized sidewall. The sidewall morphology is consistent with models of spatially random etching up to a cutoff length scale. The cutoff length scale is ≈ 5 times the size of a single deprotection volume, suggesting that collective phenomena are responsible for observed LER.

## 1. INTRODUCTION

Control of line edge roughness (LER) in future resists requires a fundamental understanding of solubility switching mechanisms and resist-developer interactions. LER depends on a number of processing parameters including the form of the aerial image, resist sensitivity, and the complex interaction of the developer (or plasma) with the spatial variation of resist solubility at the pattern edge.[1-4] For chemically amplified resists (CARs), the first step of imaging generates acid from the exposure of photoacid generators (PAG). Subsequent diffusion and reaction, catalyzed by the acid, of the polymer matrix alters its solubility in the developer solution. The distribution of acid before the post exposure bake (PEB) is controlled by the aerial image. In the limit of a sharp aerial image, a sharp concentration gradient in photogenerated acid exists at the pattern edge. Acid diffusion in this limit can result in significant roughening and loss of dimensional control.[5] Increased aerial image spread reduces the gradient in acid concentration, and acid diffusion and reaction occur within the aerial image.[6] In all cases, the primary route to deprotection is acid diffusion and its subsequent catalysis of a chemical reaction.

The connection between spatially homogeneous deprotection and minimal sidewall roughness has been suggested from observation of small LER in films with very low and very high deprotection levels.[7] Schmid et al. describe the distribution of deprotection products relative with respect to individual acid molecules. The sidewall morphology of two systems, each equivalently deprotected, depends on the overall concentration of acid. The imaged region consists of deprotection volumes defined by the spatial extent of the deprotection products created by each acid. Formed by a diffusion and reaction process, these volumes feature an internal level of heterogeneity, further compounded by the packing of the volumes. A spatial map of deprotection levels at a pattern edge is therefore a collection of these deprotection volumes (see figure 1). To illustrate this point, Schmid et al. use a molecular level simulation to create two sidewall surfaces with equivalent deprotection fractions.[7] The resultant surface morphology varies with initial acid concentration, suggesting that the level of deprotection alone is not sufficient to describe the ensuing morphology. However, spatial homogeneity is difficult to control experimentally without changes in other parameters such as developer concentration and initial acid concentration.

Advances in Resist Technology and Processing XX, Theodore H. Fedynyshyn, Editor,
Proceedings of SPIE Vol. 5039 (2003) © 2003 SPIE · 0277-786X/03/$15.00

Sidewall roughness is often represented as an average root-mean-squared (RMS) roughness, however the value of RMS roughness is known to depend on the length scale of observation. At this time, it is not clear that a general form of surface morphology exists for CARs. He and Cerina characterized the length scale dependence of observed LER as following a power law at small length scales.[7] For large scales, RMS roughness is scale invariant. This is in contrast to reports of Wunnicke et al. who observe behavior consistent with a Gaussian form.[9] For 248 nm resists, the form observed by He and Cerina appears general. This form is captured using a Fourier transform of a topographic image of the sidewall surface and appropriate windowing techniques (see figure 2).[9] The power law dependence of roughness at large length scales suggests the application of fractal mathematics to describe sidewall topology, where the slope on logarithmic axes is proportional to the fractal dimension of the surface, $D_f$. Observations of both increasing and decreasing fractal dimensions are reported for CARs in the limits of low dose, however $D_f$ consistently plateaus at large doses.[7,10] Surface fractal dimensions scale from 2 (ideal flat plane) to 3 (space-filling). Increasing $D_f$ represents increasingly heterogeneous surfaces. For CARs, the material origin of $D_f$ is not well understood. The transition between fractal and length-scale independent scaling indicates a cutoff of correlation in the formation of the surface morphology. The location of a correlation cutoff is often central to theories of surface formation.[11] We propose that the origin of this cutoff is in part due to the packing of the deprotection volumes associated with individual acid molecules. In this model, the form of deprotection establishes the length scale of heterogeneity of the surface.

We provide results on the form of the deprotection volume created within a model photoresist polymer matrix using Small Angle Neutron Scattering (SANS). For a model resist polymer and PAG, the resulting volume is heterogeneous and characterized as following Brownian motion. These studies are supplemented with topological data of model sidewall morphology created in the limit of a perfect aerial image. The size and form of the deprotection volume are compared to the form of the sidewall morphology.

## 2. EXPERIMENTAL

### 2.1 PHOTORESIST WITH DILUTE ACID

Deprotection volume studies were conducted on films of partially deuterated poly(p-tert-butoxycarboxystyrene) (d-PBOCST) ($M_{r,n}$ = 21000, polydispersity = 2.1). Here, all hydrogens on the pendant tert-butoxycarboxyl group are isotopically substituted with deuterium, while hydrogens on the backbone and styrene ring remain. Synthesis of the d-PBOCST is described elsewhere.[12] The photoacid generator, di(t-butylphenyl) iodonium perfluorooctanesulfonate (PFOS) acid, was obtained from Day Chem.[13] Solutions of d-PBOCSt were prepared with varying loadings of added PFOS, where the total PFOS content was always < 1 % mass fraction. Films were spin cast from solution in propylene glycol methyl ether acetate (PGMEA) onto SEMI-standard 75 mm diameter wafers. The d-PBOCSt / PFOS films were blanket exposed to ultra-violet radiation from a broadband source ranging between (220 and 260) nm with a total dose of 500 mJ/cm$^2$. Each film was subsequently baked on a hotplate at [90 ± 1] °C for times ranging from [0 to 600] s.[14] The resulting deprotection level was then determined as a function of PEB time with Fourier transform infrared (FTIR) spectroscopy. A minimal mass fraction of PAG required to initiate measurable deprotection levels was determined to be ≈ 0.5 %. This level is significantly higher than would normally occur in air controlled fabrication lines. Therefore, we consider only the mass fraction of acid above a baseline contamination level. Based on these measurements, processing conditions were chosen to provide a significant level of deprotection ([30 ± 5] %) from a minimal concentration of acid ([0.2 ± 0.01] % added mass fraction PFOS). A series of 22 nominally identical films were cast and processed with a post apply bake (PAB) of [120 ± 1] ºC for [30 ± 2] s, exposure energy of 100 mJ/cm$^2$, and PEB at [90 ± 1] °C for [120 ± 2] s. A second set of 22 films with no added PFOS was processed under the same conditions.

Small Angle Neutron Scattering (SANS) measurements were performed at the NIST Center for Neutron Research on the NG-1 8 m SANS beamline. To reduce background scattering, all windows were removed prior to measurement between the sample and detector, and the sample chamber was evacuated of air. Samples were measured at room temperature, with an average measurement time of 12 hours per sample. Initially, data were reduced by subtracting background measured from a stack of 22 clean silicon substrates, with corrections for detector sensitivity and dark current contributions. Intensity is placed on an absolute scale through comparisons of the direct beam flux through the samples as

compared to that measured through vacuum, and further normalized by sample volume. The 2-dimensional data is then circularly averaged. In order to extract the scattered intensity due only to the deprotection volume, the intensity resulting from the "protected" samples (i.e. no added PFOS) is subtracted from that of the partially deprotected samples. The resulting form factor is schematically depicted in figure 3.

### 2.2 PROTECTED/DEPROTECTED BILAYERS

Bilayer samples were created by spin casting d-PBOCST from solution in PGMEA (Aldrich) on silicon substrates. After baking for [90 ± 2] s on a [130 ± 1] ºC hotplate to remove residual solvent, a top layer of poly(hydroxystyrene) (PHOST) was loaded with [5.0 ± 0.1]% mass fraction PFOS was spin cast from solution in 1-butanol (Aldrich). The poly(hydroxystyrene) (PHOST) ($M_{r,n}$ = 5260, $M_{w,n}/M_{r,n}$ = 1.12 as measured by GPC), was purchased from Triquest, Inc. The bilayer was then exposed with a dose of [1000 ± 50] mJ/cm2 broadband UV radiation to generate acid in the deprotected top layer. Post exposure baking was applied for varying times at [110 ± 1] ºC. After baking, the samples were developed by immersion in 0.26N tetramethylammonium hydroxide (TMAH) for 30 s, followed by a rinse with deionized water. Silicon wafers were SEMI standard (≈ 0.5 mm in thickness) and of diameter ≈ 150 mm. Surface images were collected on a Digital Dimension 3000 atomic force microscope (AFM) in tapping mode. Fourier transforms are averaged over more than 20 images to reduce statistical noise.

## 3. RESULTS

In figure 4, the scattered intensity from a partially deprotected d-PBOCSt sample is plotted as a function of scattering vector, q. The scaling of the data at high q follow a power law of the form $I \sim q^{-D_{f,deprot}}$, where $D_{f,deprot}$ is the fractal dimension of the deprotection path. A fit to the data over the range q = [0.08 to 0.11] $Å^{-1}$ yields $D_{f,deprot}$ = [2.2 ± 0.4]. An ideal random walk possesses a fractal dimension of 2, indicating that the radius of the random walk volume grows as $N^{1/2}$, where N is the number of steps in the walk. In contrast, a compact, space-filling walk would scale as N. The deprotection path can be described as a random walk and therefore does not fill space efficiently. As a result, the interior volume of the deprotection volume is inhomogeneous with local areas of larger or smaller levels of deprotection.

Further information on the size and interactions of the deprotection paths are obtained from the correlation length, ξ. Here, ξ represents a distance of interaction of the deprotection path. In the limit of non-overlapping deprotection paths, ξ is approximately equal to the size of the deprotection volume. In figure 5, the data are presented as inverse intensity vs. $q^2$ and fit to a line. The correlation length is obtained from the ratio of the slope and the intercept, where ξ = [12 ± 1] nm. The random walk scaling suggests the use of the Kratky limit as a more direct determination of deprotection volume size. In the limit $qR_{G,deprot} >> 1$, $Iq^2$ is a constant. The data at lower q in figure 6 follow a typical Kratky form. Data in the region q > 0.06$Å^{-1}$ suffer from an overestimation of the background subtraction, making a precise determination of $R_{g,deprot}$ difficult. Using the q value of maximum $Iq^2$ indicated in figure 6, we estimate $R_{G,deprot}$ (= [11.1 ± 3] nm). This value is consistent with the correlation length obtained from the Ornstein-Zernike analysis.

Topological data from tapping mode atomic force microscopy of a bilayer deprotected/protected polymer pair after processing and development are presented in figure 7. The data are consistent with the form observed by He and Cerina, with two approximately linear regimes and a crossover at intermediate q. The slope of the linear regime is consistent with a slope of ≈ 2, however the limited regime of linearity between the crossover and the background noise at high q prevent an accurate extraction of this quantity (what quantity?). The data of figure 7 are recorded for varying PEB times. In general, the form of the morphology was independent of PEB time and temperature. This is in contrast to prior data taken from the same system with a much slower temperature ramp. The constancy of the morphology suggests that the form is created at early bake times. If we designate the location along the q axis of the correlation cutoff as $q_{cutoff}$, the corresponding real space characteristic length, $d_{cutoff}$, is obtained from the relationship $q_{cutoff}=2\pi/d_{cutoff}$. An approximate value of the correlation cutoff is $d_{cutoff} \approx$ [30 ± 5] nm.

## 4. DISCUSSION

The form of the deprotection volumes created here in the limit of dilute acid concentrations is characterized as following a Brownian motion. The diffusion and catalyzed deprotection reaction by the acid is isotropic. This result suggests the deprotection reaction path is not restricted by previously visited regions. The volume encompassing the random walk path is heterogeneous with internal spatial variations of deprotection level. On average, the volumes are characterized as blobs with a maximum in deprotection near the center decaying to the average resist composition at the edges. The characterization of the deprotection path as "Brownian" does not necessarily prove Fickian acid diffusion. The diffusion-reaction process of photogenerated acids is complex withnumerous side reactions and volatile by-products that can change the surrounding matrix.[16-20] The quantities measured here only characterize the final path of deprotection in a limit of dilute acid.

The resulting sidewall is then characterized as "fuzzy blobs" that pack in a manner dependent on the initial concentration of acid. Acid distribution is controlled by PAG chemistry and optical imaging conditions, such as initial PAG concentration, aerial image, and chromophore efficiency. Blob size is determined by material factors, including the PEB temperature and time, glass transition temperature of the resist, activation energy of the PAG, and the deprotection reaction efficiency. The size and form of the deprotected volume may be controlled with current resist components. The use of copolymers in resists could impact the form significantly, where acid mobility is reduced or enhanced in the co-monomer phase, restricting diffusion to local regions of protected polymer. In contrast, a random dispersion of base quencher is not expected to alter the form. Instead, added base should restrict the overall path length and provide a smaller volume of similar heterogeneity.

The form of the power spectrum shown in figure 4 follows a power law at high q with a characteristic length cutoff at $d_{cutoff} \approx$ [25 to 30] nm. The cutoff is consistent with the apparent "grain size" in the image of figure 1. Based on prior measurements of the molecular dimensions in thin film resists, the cutoff length is estimated as $d_{cutoff} \sim$ [9 to 10] $R_{G,poly}$, where $R_{G,poly}$ is the radius of gyration of the polymer molecules in the resist. In the power law regime, the precise extraction of a power law is difficult due to the small range of measured frequencies, the convolution of the probe tip shape with the surface structure, and a lack of precision in determining background signals in AFM data. The application of scattering techniques can overcome some of these issues, however the small size of the roughness here makes the scattering volume, and hence the signal-to-noise ratio, extremely small. In general, the power law regime is very insensitive to a variety of processing factors including a wide range of PEB times and temperatures.

Based on the form of the deprotection volume, we can calculate an effective diffusion-reaction coefficient of the acid. As an approximation, we assume that the time to reach the PEB temperature is much smaller than the overall PEB time, allowing the use of the PEB time as the acid diffusion time. The random walk form suggests (but not uniquely) a Fickian representation of $R_{G,deprot} = (2D_{deprot}\, t)^{0.5}$, where t = 60 s, $R_{G,deprot}$ = 12 nm, and $D_{deprot}$ is a coefficient of diffusion-reaction for the acid. The resulting value of $D_{deprot}$ ($\approx$ 1e-14 $cm^2/s$) is consistent with prior results using a model bilayer. For an order of magnitude approximation of $R_{G,deprot}$ under different processing conditions, $D_{deprot}$ is assumed to be independent of temperature. Applying $D_{deprot}$ to the conditions used in the bilayer, where t = 90 s, the predicted value of $R_{G,deprot}$ = 5 nm is consistent with estimates from modeling in a different CAR. The size scale of the average deprotection volume associated with a single acid is therefore inconsistent with the cutoff length scale, where $d_{cutoff} \approx$ [5 to 6] $R_{G,deprot}$. The surface of a sidewall cannot be simply described as closely packed, impenetrable deprotection volumes. The larger size of the cutoff length scale suggests that multiple deprotection volumes collectively interact to create the observed morphology. Further description may require insight into potential collective phenomena within the diffusion-reaction process or physical effects due to developer-resist interactions.

## 5. CONCLUSIONS

The form of the average deprotection volume created by well-dispersed acid molecules is determined using Small Angle Neutron Scattering (SANS). The form is consistent with a simple random walk with an effective diffusion-reaction

coefficient on the order of 1e-14 $cm^2/s$. Within this volume, the level of deprotection varies spatially. On average, a maximum in deprotection occurs at the center of the volume, decaying to a background level at the edges. The volume is therefore described as a "fuzzy blob" and the interior of an imaged resist is considered to be a distribution function of fuzzy blobs. The final form of LER was not consistent with a simple model of individual, non-interacting and non-overlapping fuzzy blobs, indicating the need for further model refinement and the incorporation of developer-resist interactions.

## ACKNOWLEDGEMENTS

This work was funded in part by the DARPA Advanced Lithography Program under contract N66001-00-C-8803. Additional funding was provided by the NIST Office of Microelectronic Programs. R. L. J. and V. M. P. are supported by a National Research Council-NIST postdoctoral fellowship.

## REFERENCES


1. F. A. Houle, W. D. Hinsberg, M. I. Sanchez, J. A. Hoffnagle, "Influence of resist components on image blur in a patterned positive-tone chemically amplified photoresist", J. Vac. Sci. Technol. B 20, 924-931, 2002.
2. J. F. Cameron, S. L. Ablaza, G. Xu, W. Yueh, "Impact of Photoacid Generator Structure on DUV resist performance" Proc. SPIE, 3678, 785-799, 1999.
3. G. P. Patsis, A. Tserepi, I. Raptis, N. Glezos, E. Gogolides, E. S. Valamontes, "Surface and line-edge roughness in solution and plasma developed negative tone resists: experiment and simulation", J. Vac. Sci. Technol. B 18, 3292-3295, 2000.T. Yoshimura, h. Shiraishi, J. Yamamoto, S. Okazaki "Nano edge roughness in polymer resist patterns", Appl. Phys. Lett. 63, 764-768, 1993.
4. T. Yamaguchi, H. Namatsu, M. Nagase, K. Yamazaki, K. Kurihara, "Nanometer-scale linewidth fluctuations caused by polymer aggregates", Appl. Phys. Lett. 71, 2388-2390, 1997.
5. E. Dobisz, T. N. Fedynyshyn, D. Ma, L. M. Shirey, R. Bass, "Electron-beam nanolithography, acid diffusion, and chemical kinetics in SAL-601", J. Vac. Sci. Technol. B 16, 3773-3778, 1998.
6. W. D. Hinsberg, F. A. Houle, G. M. Poliskie, D. Pearson, M. I. Sanchez, H. Ito, "Product Volatalization as a Probe of the Physics and Chemistry of Latent Image Formation in Chemically Amplified Resists" J. Phys. Chem. A 106, 9776-9787, 2002.
7. G. M. Schmid, M. D. Smith, C. A. Mack, V. K. Singh, S. D. Burns, C. G. Willson, "Understanding Molecular Level Effects during Post Exposure Processing", Proc. of the SPIE, XXXXXX
8. D. He and F. Cerrina, "Process dependence of roughness in a positive-tone chemically amplified resist", J. Vac. Sci. Technol. B 16, 3748-3751, 1998.
9. O. Wunnicke, A. Hennig, K. Grundke, M. Stamm, G. Czech, "Surface properties and topography of 193 nm resist after exposure and development", Proc. SPIE XXXXXX
10. M. Ishida, K. Kobayashi, J.-I. Fujita, Y. Ochiai, H. Yamamoto, S. Tono, "Investigating Line-Edge Roughness in Calixarene Fine Patterns Using Fourier Analysis", Jpn. J. Appl. Phys. 41, 4228-4232, 2002.
11. V. Constantoudis, E. Gogolides, B. P. Patsis, A. Tserepi, E. S. Valamontes, "Characterization and Simulation of Surface and Line-Edge Roughness", J. Vac. Sci. Technol. B 19, 2694-2698, 2001.
12. D. A. Kessler, Zvi Ner, and L. M. Sander, "Front propagation: precursors, cutoffs, and structural stability", Phys. Rev. E. 58, 107-114, 1998.
13. E. K. Lin, C. L. Soles, D. L. Goldfarb, B. C. Trinque, S. D. Burns, R. L. Jones, J. L. Lenhart, M. Angelopoulos, C. G. Willson, S. K. Satija, W.-L. Wu, "Direct measurement of the reaction front in chemically amplified resists", Science 297, 372-375, 2002.
14. Certain commercial equipment and materials are identified in this paper in order to specify adequately the experimental procedure. In no case does such specification imply recommendation by the National Institutes of Standards and Technology nor does it imply that the material or equipment specified is necessarily the best available for this purpose.
15. The data in this manuscript, in the figures, and in the tables are presented along with the standard uncertainty (±) involved in the measurement, where the uncertainty represents one standard deviation from the mean.
16. R. L. Jones, V. M. Prabhu, D. L. Goldfarb, E. K. Lin, C. L. Soles, J. L. Lenhart, W.-L. Wu, M. Angelopoulos, "Correlation of the reaction front with roughness in chemically amplified resists", in "Polymers for Micro- and nano-electronics", ACS Symp. 2003.
17. W. D. Hinsberg, F. A. Houle, M. I. Sanchez, G. M. Walraff, "Chemical and physical aspects of the post-exposure baking process used for positive-tone chemically amplified resists", IBM J. Res. & Dev. 45, 667-682, 2001.
18. R. Ichikawa, M. Hata, N. Okimoto, S. Oikawa-Handa, M. Tsuda, "Acid-catalyzed deprotection mechanism of tert-butoxycarbonyloxy polymers in chemically amplified resists", J. Polym. Sci. A Polym. Chem. 36, 1035-1042, 1998.
19. M. D. Stewart, H. V. Tran, G. M. Schmid, T. B. Stachowiak, D. J. Becker, C. G. Willson, "Acid catalyst mobility in resist systems", J. Vac. Sci. Technol. B 20, 2946-2952, 2002.
20. X. Shi, "Effect of coulomb interaction and pKa on acid diffusion in chemically amplified resists", J. Vac. Sci. Technol. B 17, 350-354, 1999.

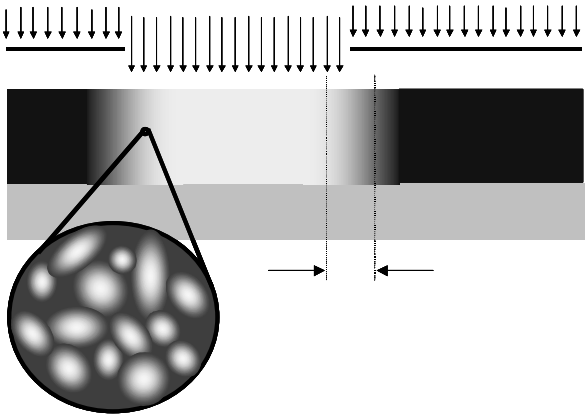

Figure 1. Schematic of an image in a chemically amplified resist. The imaged region (bright) features aerial image blur (gradient into dark region) that creates a gradient in acid concentration. Within the gradient, acid diffusion creates a spatially heterogeneous pattern of deprotection, characterized as a series of "fuzzy blobs".

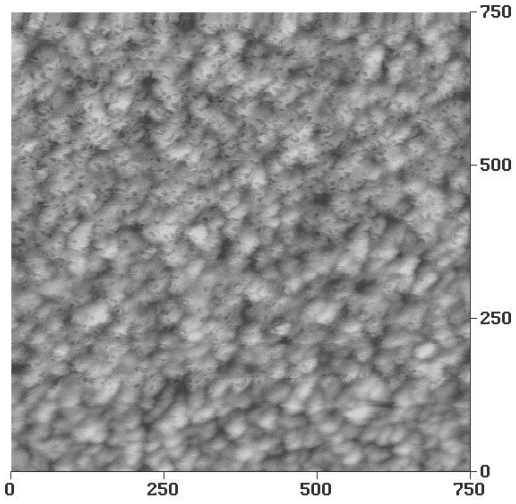


Figure 2. Topography indicative of the roughness observed at a patterned edge in CA resists. Shown is topographic data from AFM of a bilayer after a 90 s PEB, bright regions are elevated. Total height scale is 20 nm, and image is 750 x 750 nm. Root mean squared value of roughness is 2.1 nm.

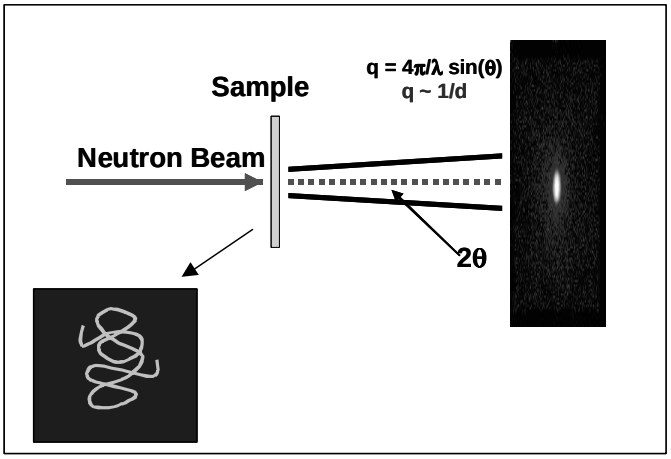


Figure 3. Schematic of the SANS geometry. Also shown is the hypothetical real space image of a random walk deprotection path (bottom left) that results from the background subtraction described in the text.

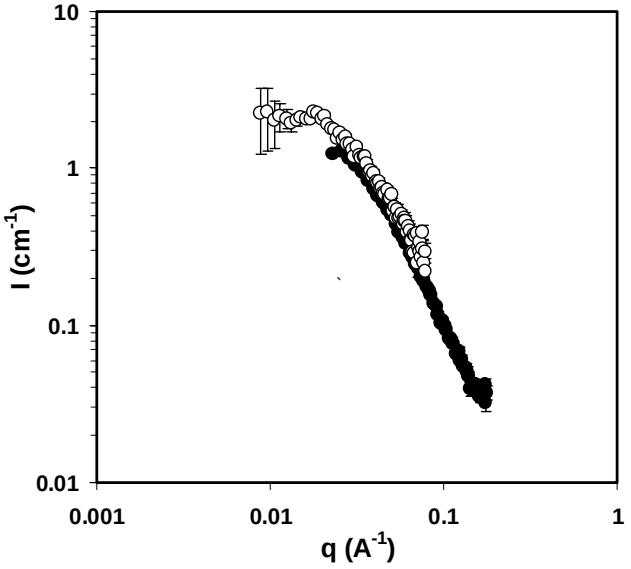


Figure 4. Data from a partially deprotected d-PBOCST film plotted as scattered intensity vs. scattering vector, q. Shown are data from SANS measurements at two configurations emphasizing low q (white circles) and large q (filled circles).

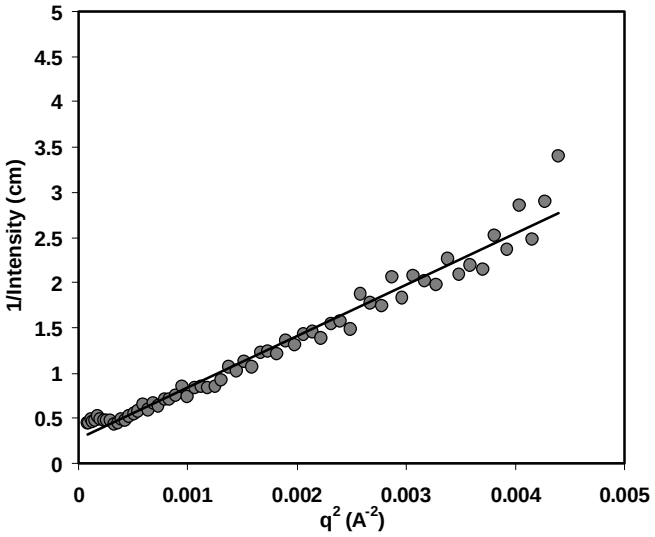


Figure 5. Data from a partially deprotected d-PBOCST film plotted in Ornstein-Zernicke form. Shown are data from SANS measurements plotted as inverse intensity as a function of $q^2$ (solid circles). A linear fit to the data is shown as the solid line.

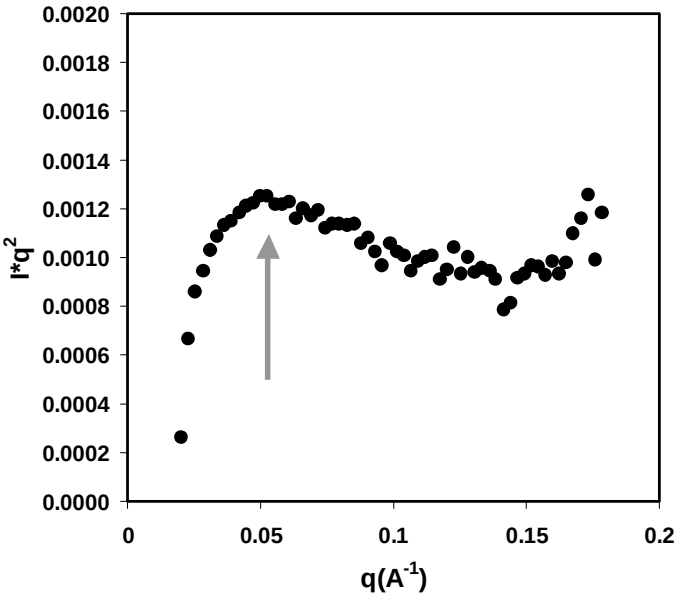


Figure 6. Kratky plot of $Iq^2$ vs. q. Shown is data from a partially deprotected sample in the limit of dilute acid concentration. The arrow indicates the approximate location of the maximum value of $Iq^2$ described in the text.

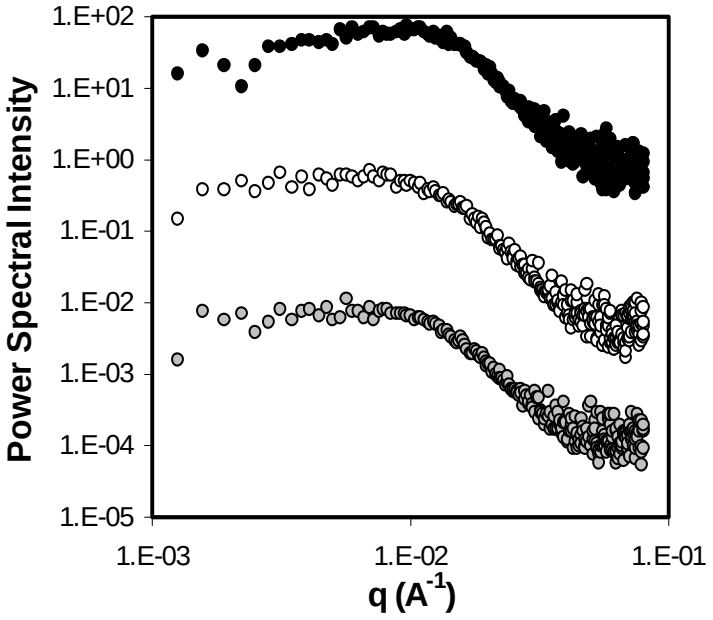


Figure 7. Power spectral intensity from bilayers after varying amounts of PEB time. Shown are data from PEB times of 15 s (solid circles), 60 s (white circles), and 180 s (greyed circles). The intensities are shifted for clarity.